REGULAR PAPER

Improving the Industrial Efficiency of Recycling Aluminum Alloy Chips Using Friction Stir Extrusion: Thin Wires Production Process

Gianluca Buffa[1] · **Davide Campanella**[1] · **Muhammad Adnan**[1] · **Umberto La Commare**[1] · **Giuseppe Ingarao**[1] · **Livan Fratini**[1]

Abstract

Friction stir extrusion is one of the most promising solid-state chip recycling techniques because of its relative simplicity and high efficiency. One of the most straightforward applications for the process is the production of recycled wires to be utilized as filler material in welding or welding-based additive manufacturing processes, in order to create an industrial symbiosis link, fostering a circular economy and enhancing the technology readiness level of the process. The scalability of the process to the thin wires needed for such applications has not been investigated so far. In this paper, an experimental and numerical analysis was developed. A dedicated numerical model was first validated and then used to design the tool geometry. The effect of tool rotation and tool force on both "standard" mechanical properties, as Ultimate Tensile Strength and microhardness, and specific properties for the envisaged application, as the wrapping around reels with different radii, was investigated. The numerical model results were used to explain the influence of the process parameters on the material flow as well as on the distribution of the primary field variables, namely temperature, strain, and strain rate. Finally, the energy demand was measured, and the specific energy consumption (SEC) was evaluated. It was found that a conical shoulder surface favors the conditions for effective solid bonding. Low values of the extrusion force have detrimental effects on the wires properties as they result either in insufficient strain, or hot cracking defects. High values of extrusion force results in lower SEC, unlocking the potential of the process as symbiotic link enabler.

Keywords Solid state · Recycling · Aluminum alloys · FEM

Abbreviations

TRL	Technology readiness level
UTS	Ultimate tensile strength
ECAP	Equal channel angular pressing
FSE	Friction stir extrusion
ShAPE	Shear assisted processing and Extrusion process
CFD	Computational fluid dynamics
SPH	Smoothed particle hydrodynamics
CAE	Computer-aided engineering
HV	Hardness value
FEA	Finite element analysis
FSW	Friction stir welding
SEC	Specific energy consumption

✉ Gianluca Buffa
    gianluca.buffa@unipa.it

1   Department of Engineering, University of Palermo, Viale
    Delle Scienze, 90128 Palermo, Italy

1 Introduction

Approximately 21% of the energy needed worldwide is used for the manufacture of materials and it is responsible for about 25% of the world's CO_2 emissions. In particular, metal production accounts for about 8% of the world's total energy consumption [1]. Since 1971, steel demand worldwide has increased threefold, primary aluminum nearly sixfold and plastic more than tenfold, making it imperative to find a strategy that can separate economic growth from resource depletion [2, 3]

Light alloys have been intensively used in the manufacturing industry over the last few decades due to their ability to allow weight reduction while improving the mechanical performance of structures. Using these alloys, recycling can save up to 90% of energy compared to primary production [4, 5]. Considering these benefits, there is still room to improve the efficiency and resource usage of the recycling process. Traditional recycling processes of chips are based on the remelting of the material [6]. This process is

2 Springer KSPE

energy-intensive, and it is characterized by significant permanent material losses. One of the main causes of material loss is the formation of oxides, which is facilitated by the melted material's high temperature. The last aspect is particularly important when aluminum alloy machining chips are taken into account, because of both the affinity of this material with oxygen and the high ratio surface/volume of the chips. Problems with material remelting can be overcome by applying solid-state recycling techniques [7] which allow for significant savings in the energy required for the recycling process [8]. Among the most used and effective techniques, there are hot extrusion [9], Equal Channel Angular Pressing (ECAP) [10], and Spark Plasma Sintering which, unlike the previous processes, is not based on severe plastic deformation but rather on powder metallurgy [11].

Other approaches are based on a combination of processes to get fulkly consolidated semifinished products: [12] suggested a combination of extrusion and rolling to obtain flat. Cooper et al. [13] proposed chips extrusion as a preparatory step to remelting.

As far as the powder metallurgy-like approach: Koch et al. [14] proposes a recycling process made of a field-assisted sintering (FAST) process to consolidate the aluminum alloys chips, and a forward rod extrusion process.

The energy efficiency of such process category with respect conventional remelting processes has been already proved. Duflou et al., by developing a full Life Cycle Assessment analysis, observed a significant environmental impact reduction in aluminium alloys recycling processes, such reduction id mainly due to the lack of permanent material losses occurring during remelting [15].

One of the most promising solid-state processes for chip recycling is Friction Stir Extrusion (FSE). Although it was patented in 1993 by TWI as a modification of Friction Stir Welding, only in the last few years researchers have started to investigate the process and its potential. FSE can be used for every light alloy or steel. However, most of the papers in the literature are focused on aluminum alloys due to the larger use of these alloys for industrial applications [16]. One of the first attempts to use FSE as a recycling technique was made by Tang and Reynolds [17]. In their paper, the authors started from AA2050 and AA2195 machining chips to produce 2.5 mm wires. They found that sound wires can be produced, although higher extrusion rates must be used to increase the process's industrial appeal. Behnagh et al. [18] highlighted the wires defects due to both cold crack and hot crack occurring during FSE of AA7277 wires, 6 mm in diameter. The authors highlighted that, with proper process parameters, mechanical properties comparable to the ones of the parent material can be reached in the extruded wires. Tahmasbi et al. [19] focused on the corrosion resistance properties of AA7022 wires produced starting from machining chips.

The authors found that corrosion resistance decreases as heat input, i.e., tool rotation, increases. Very recently, Li et al. [20] highlighted the process mechanics of FSE by experimentally measuring strain and strain rate through the use of a proper marker. The results show how the process parameters influence the deformation zone and the "dead zone", but also highlighted how, in order to fully understand the complex material flow occurring during the process, further analyses are needed. Finally, Kalsar et al. [21] studied the mechanical and microstructural properties of 5 mm wires produced by Shear assisted processing and Extrusion process (ShAPE). The authors highlighted how the peculiar microstructure developed in the wires enhances and speeds up the post-processing heat treatments on the products.

Concerning the environmental sustainability aspect of FSE processes, some of the authors of the present paper have quantified the energy efficiency of this process with respect conventional processes [22]. In this paper it is reported that the reduction in Primary Energy demand is due the (1) lack of permanent losses (oxidation during remelting) and (2) the reduced number of process steps to turn chips into wires. Concerning the latter aspect, FSE allows the wire drawing process (a very high energy demanding process) to be skipped enabling substantial primary energy savings.

As far as the numerical simulation of the FSE process is regarded, only a very limited number of papers can be found in the literature. As for Friction Stir Welding, two main approaches can be used: (1) CFD based and (2) solid mechanics based. The research group guided by prof. Reynolds at University of South Carolina has been one of the most active in this field during the last few years. One of the first papers presenting a dedicated numerical model for FSE is the one by Zhang et al. [23]. A CFD model was proposed, able to provide insights on the complex material flow occurring during the process through the prediction of strain, strain rate and particles path lines. Later, a thermal model was presented by the same research group with the aim to predict the evolution of temperature during the process [24] and, finally, a comprehensive model able to consider both the evolution of temperatures and the material flow was proposed [25]. Recently, Li et al. [26] presented a smoothed particle hydrodynamics (SPH) based numerical model. The mesh-free approach, after proper validation, was used to successfully predict material flow, temperature, and extrusion forces. As conventional solid mechanics based models are regarded, some of the authors of the present paper developed a dedicated model for FSE of Mg alloys able to predict the occurring material flow, temperature, strain, and strain rate distribution, as well as the occurrence of solid bonding in line with the primary process factors (tool rotation and extrusion force on tool) [26, 27]. Finally, Behnagh et al. [28] presented a coupled solid mechanics—cellular

automation model to predict the complex microstructural evolutions occurring during the process.

From the literature analysis reported above, it arises that all the studies focus on the production of "wires" or rods with dimeter in the range of 2.5–6 mm. Although these geometries can be effective to demonstrate the process feasibility and to highlight more easily the complex process mechanics and microstructural evolutions, they are of less interest for industrial applicability with respect to thin wires. Thin wires can be used for a variety of applications, including electrical ones and as fillers in arc welding and arc welding based additive manufacturing processes. In fact, wires and cables account for about 8% of the whole semi-manufacturing aluminum production [29, 30].

On the other hand, the possibility to activate industrial symbiotic link between chips recycler and companies using the recycled semi-finished product as material input is still to be fully explored. In this respect, potential link can be activated if the metallic wire-based AM technologies are considered, in fact the recycled wires obtained by FSE could be used, for instance, as input material for wire based additive manufacturing processes.

In particular, an integrated approach for combining arc additive manufacturing and a direct chip recycling process based on FSE for lightweight alloys, implementing such Hybrid Manufacturing process into a cost effective manufacturing route, would allow manufacturers to repair worn part and produce new complex components with zero defects, high metallurgical quality and high productivity rates, while at the same time ensuring maximum material efficiency and a minimized overall consumption of material and energy resources. However, the scalability of the FSE process to thin wires has not been demonstrated yet, as in this case additional difficulties arise due to the dimension of the chips which is comparable to the final wire diameter and could have detrimental effects on the wires integrity.

In this paper, the computer-aided engineering (CAE) of FSE to produce AA6082-T6 wires characterized by diameter equal to 1.2 mm is presented. The process was carried out starting from machining chips. A dedicated numerical model was first validated and then used to select proper rotating tool design. An experimental campaign was carried out with varying tool force and rotation speed, and the main mechanical properties of the wires were highlighted, including the wrapping in reels needed for transportation and use in industrial environment. The numerical model was utilized to emphasize the primary field variable distributions and connect them to the

calculated wires mechanical performance. Finally, the electrical energy demand was measured for all the considered process conditions and the Specific Energy Consumption (SEC) was calculated and compared to literature data on conventional production routes.

2 Materials and Method

2.1 Experimental Activity

AA6082-T6 aluminum alloy was used as starting material for the present study. The chips were obtained starting from a 60×40 mm bar through a milling procedure distinguished by a depth of cut of 0.5 mm, a tool rotating speed of 150 mm/min, and a tool feed rate of 200 mm/min. The diameter of the utilized mill was 63 mm. The average size of the chips produced during this process are 7 mm length, 2 mm width and 2 mm thickness. The process was carried out without cutting fluid to speed up the following operations avoiding chips cleaning. It is worth noting that in the case chips coming from industrial processes, any trace of cutting fluid must be removed before starting the FSE process in order to avoid oil contamination in the produced wire. In Tables 1 and 2 typical chemical composition and mechanical properties of the used material are reported. It should be observed that both the starting conditions of the material as the bar is considered, the T4 state and the annealed conditions are reported. It should be observed that the milling operation modifies the hardening conditions of the used material which is supposed to get the O state.

Figure 1a shows the adopted FSE fixture setup: a dedicated tooling set was manufactured in 4140 steels. The rotating tool speed, which serves as the backward extrusion die, has an exterior diameter of 14.7 mm, a center through extrusion channel that is 1.2 mm in diameter and 1 mm in height, and a broadening channel that starts at 3 mm in diameter before getting narrower again.

Table 2 Mechanical properties at room temperature of AA6082 in the O, T4 and T6 state

Heat treatment	UTS (MPa)	Elongation (%)	H_v
O	130	27	35
T4	200	14	65
T6	290	10	95

Table 1 Chemical composition % w/w of the used AA6082

Chemical composition % w/w								
Al	Cr	Cu	Fe	Mg	Mn	Si	Ti	Zn
95.2|98.3	≤0.25	≤0.1	≤0.5	0.6|1.2	0.4|1.0	0.7|1.3	≤0.1	≤0.2

Fig. 1 a FSE fixture used for the experimental campaign, **b** shoulder tool geometries, **c** cross section of the used tool with dimensions
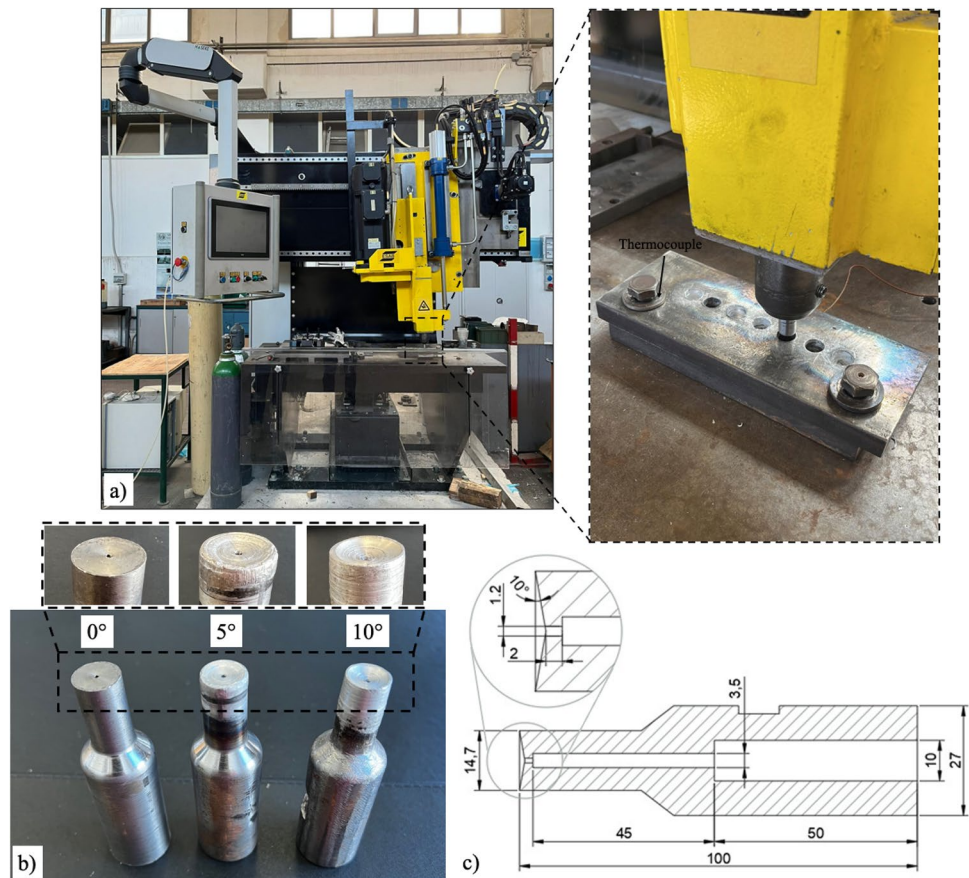

Table 3 Investigated process conditions

Tool rotation (rpm)	Force (kN)		
	15	18	21
500	ID3	ID6	ID9
400	ID2	ID5	ID8
300	ID1	ID4	ID7

Different tool shoulder surfaces were preliminary tested, namely a flat one and two conical ones with 5° and 10°, respectively (Fig. 1b). The die chamber has an internal diameter of 15 mm determining an extrusion ratio of 12.25. A thermocouple was embedded at the bottom center of the extrusion chamber for the numerical model validation. The friction stir extrusion process was carried out on a Friction Stir Welding machine ESAB LEGIO FSW 3ST operating in Z-axis force control mode. The experimental plan reported in Table 3 was carried out with three repetitions for each of the considered case studies. The considered values of tool rotating speed and applied tool force were chosen on the basis of former studies [31] and preliminary tests on the used aluminum alloy. The central point of the experimental plan was also preliminarily repeated for the considered tool shoulder angles (0°, 5°, 10°).

According to the test conditions, the rate of material extrusion changed. The numerical model's input data was obtained from the ESAB LEGIO controller's recording of the die vertical movement during the extrusion at a sampling rate of 10 Hz. Extrusions were stopped when the tool was about to reach the bottom of the die chamber, namely when the entire material inside the chamber, i.e. the chips, were extruded; in this way an average length of extruded wire of about 500 mm was reached. Specimens were taken from each of the completed case studies in order to evaluate the mechanical and microstructural features of the wire material condition. Tensile testing was conducted in accordance with ASTM D2256 specifications. For each case study, three tests were taken into account. To highlight microstructures, cross sections of the wires were cold mounted, polished, and etched for 15 s with Keller's reagent (190 ml H_2O, 5 ml HNO_3, 3 ml HCL, and 2 ml HF). Vickers microhardness testing was done along the cross-sectional diameters of the samples.

Finally, in order to measure the ductility of the produced wires, bending tests were carried out for different values of the bending radius, namely 15, 12.5, 10, 7.5 and 5 mm (Fig. 2). Such test was aimed to verify the possibility to wrap the obtained wire around a reel for actual industrial applications.
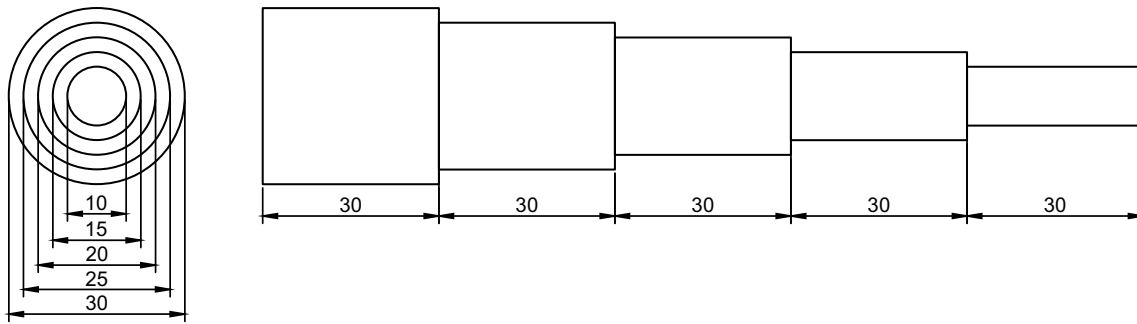
Fig. 2 Bending "reel" test fixture

2.2 Numerical Model

About the numerical model of the researched FSE process, it was created using the commercial FEA program DEFORM3DTM, which is a Lagrangian implicit code specialized for metal forming processes. It should be observed that even if the chips should be considered a discrete compound, they were modelled as a single workpiece. Moreover, the Shima and Oyane yield surface for porous materials was employed to account for the real density of the agglomeration. The AA6082 chip billet was modeled as one porous object with an initial relative density of 0.6; this value was determined by dividing the density of the base material by the density of the compacted billet. Yet, the executed numerical simulations demonstrated that, prior to the extrusion process, the density of the chips billet quickly grew to 1 [32]. As the single element reaches the full density (i.e. density equal to 1), a rigid-visco-plastic approach with Von Mises yield criterion and associated flow rule is then applied.

The material database JMatPro demo and internal tests utilized the following material model:

$$\sigma = k\varepsilon^n \dot{\varepsilon}^m \exp\left(\frac{\beta}{T}\right) \tag{1}$$

where k = 6.616, n = 0.0368, m = 0.0759, and β = 1504 are constants specific of the considered material; ε, $\dot{\varepsilon}$ and T are the effective strain, effective strain rate, and temperature, respectively. The thermal problem was linearized to speed up the simulation by using constant thermal conductivity and thermal capacity, which are equivalent to 180 N/(s K) and 2.4 N/(mm^2 K), respectively. This approach has already been proven effective for FSW processes [33]. The contact between the tool and the workpiece was model through the shear friction model, characterized by a friction factor of 0.4, and heat exchange coefficient of 11 N/m (mm Ks). Some of the authors got these results from a prior numerical campaign of FSW of aluminum alloys [34].

For the only purpose of the thermal study, the spinning tool and the extrusion chamber were represented as rigid bodies and meshed with about 28,000 and 26,000 tetrahedral elements, respectively. Around 18,000 tetrahedral elements were chosen to mesh the workpiece, with a finer mesh near the extrusion channel having an average dimension of 0.3 mm. These values were chosen based on a preliminary sensitivity analysis aimed to reduce the number of elements as much as possible preserving model accuracy. Figure 3 shows the model at the beginning of the simulation. In an effort to lessen the CPU time needed for each simulation, the tool movement was controlled with assigned stroke vs time data taken from the experiments as described in the previous paragraph.

The model was tuned using experimental temperature measurements with a thermocouple placed at the bottom of the die chamber on the symmetry axis during preliminary experiments.
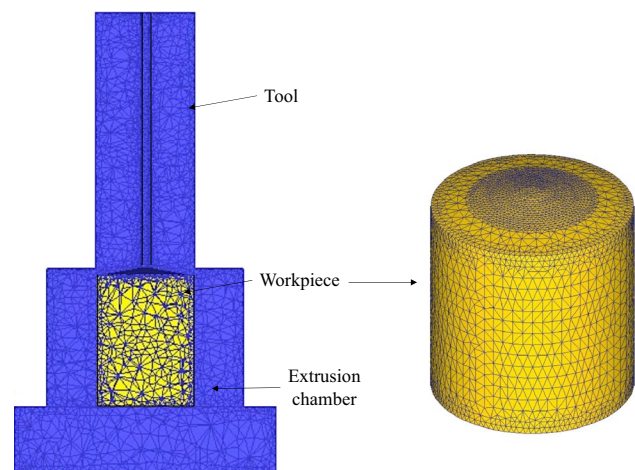

Fig. 3 Sketch of the numerical model at the beginning of the simulation

Fig. 4 Temperature at the bottom center of the billet during the process for case study 9 (exp vs num)
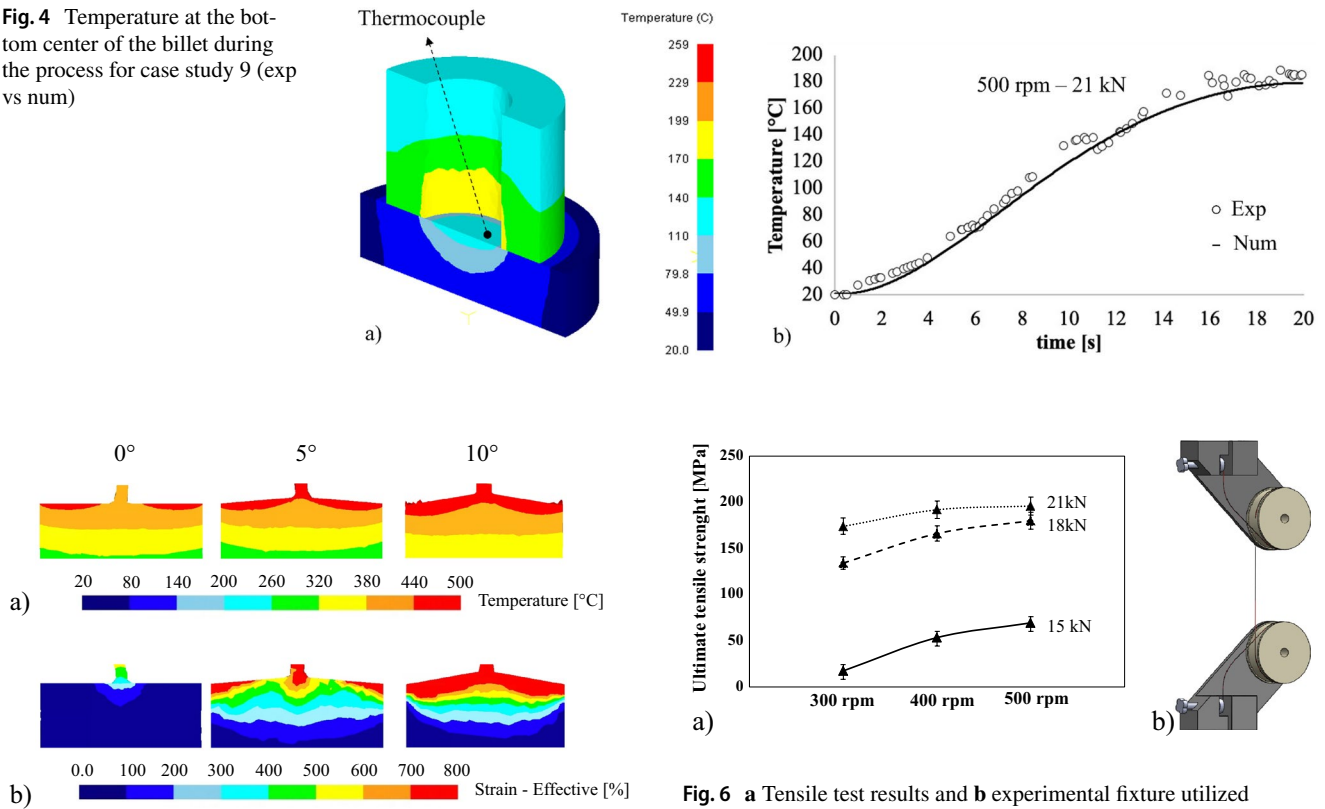

Fig. 5 Temperature and effective strain distribution in a cross-section for case study 9

Fig. 6 **a** Tensile test results and **b** experimental fixture utilized

3 Results and Discussion

3.1 Tool Design Through the Numerical Model

First, the numerical model was validated against temperature for all the considered case studies. Figure 4 shows the temperature trend during the process, as measured by the thermocouple embedded at the bottom center of the extrusion chamber and as calculated by the numerical model.

The numerical model was then used to determine the most effective tool design to be used in the experimental campaign. In particular, three different shoulder angles were tested, i.e., 0° (flat shoulder), 5°, and 10°. Figure 5 shows the temperature and effective strain distribution in a cross-section.

Increasing temperature and increasing strain can be observed with increasing shoulder angle. The inclined surface of the shoulder results in two beneficial effects: on the one hand, larger angles imply a larger surface and, hence, larger heat input; on the other hand, a conical shoulder surface promotes a material flow component toward the center of the extrusion which enhances material mixing and solid bonding. Additionally, the increased deformation
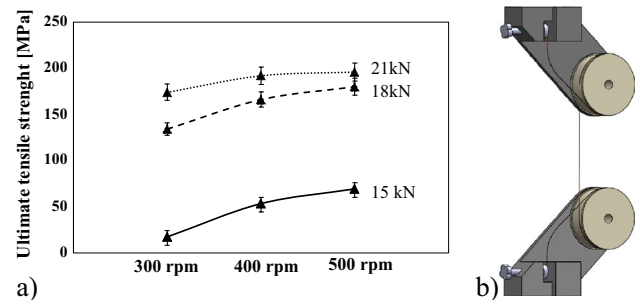
work, decaying into heat, further contributes to the temperature increase and material softening. The results above described apply to all case studies and, for these reasons, only the tool with a shoulder angle equal to 10° was considered for the subsequent analyses.

3.2 Mechanical Characterization

Tensile tests have been carried out on the obtained wires according to ASTM D2256. The average values for the case studies under consideration are displayed in Fig. 6a, and the experimental setup utilized for the experiments is shown in Fig. 6b.

It is observed that an increasing trend was obtained both with increasing tool force and tool rotation. In particular, when the tool force is equal to 15 kN maximum UTS was about 60 MPa. For tool force values equal to 18 kN and 21 kN significantly higher resistance was observed, with the best performing wires reaching about 200 MPa. It is worth noting that this value corresponds to the one of the parent materials in the T4 state, as it will be discussed in the following.

On the wires' cross section, microhardness tests were carried out. Three measurement points for each section were considered (Fig. 7b). Due to the friction forces at the interface between the shoulder and the material to be processed, a special input variable was considered as the heat flow input
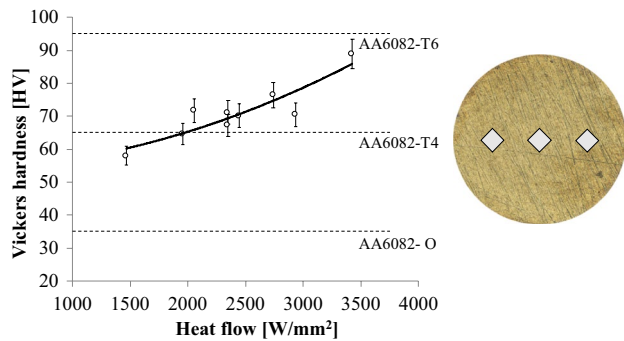
Fig. 7 **a** HV microhardness as a function of heat low and **b** sketch of the indentations

Fig. 8 **a** sound wire (case study 5) and hot cracked wire (case study 3)

in to demonstrate the results. Consideration was given to the analytical formulation put forward by Song and Kovacevic for the heat flow produced beneath the tool shoulder in friction stir welding [35]:

$$q = 2\pi\mu F_N rN \qquad (2)$$

where r is the distance between the estimated point and its axis, N is the rotational speed of the tool, μ is the Coulomb friction coefficient, assumed equal to 0.7, and F_N is the normal force.

Figure 7a shows the trend of HV, calculated as the average value of the three indentations per cross-section, as a function of the heat flow. In the graph, the microhardness of the base material in the as received conditions, i.e., T6, in the O state and in the T4 state are reported too.

A few interesting observations can be made increasing values are observed with increasing heat flow; the values obtained are between the HVs of the parent material in the T4 and T6 state. As long as the latter is considered, it can be stated that the solid bonding occurring was effective resulting in local micromechanical properties which are always better than the ones of the parent material in the O state. This finding is in line with what Baffari et al. [31], who, working with FSE of AA2050, found that, regardless of the starting alloy condition, i.e., T4 or O, the final rod showed mechanical properties close to the ones of the parent material in the T4 state. As known, T6 corresponds to artificial aging while T4 corresponds to natural aging. So, it may be said that the material's thermal cycle throughout the procedure produces an "almost" T4 heat treatment, which enhances the wire's mechanical resistance. Additionally, it is important to note that, for the considered AA6082 alloy, the T4 state allows for better ductility with respect to the T6 one. This can be an advantage when the final application of the wire is the use as filler wire in welding or welding-based additive manufacturing processes, as it can be wrapped in reels without the risk of
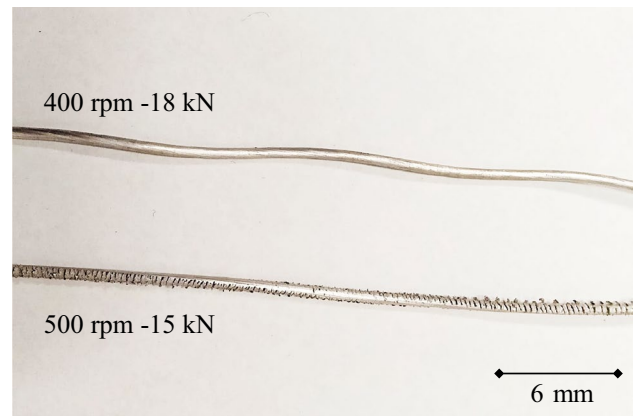
cracking. It is also noted that the UTS values shown in Fig. 6 for the best-performing wires can reach but not overcome the UTS of the parent material in the T4 state. Additionally, although the lowest UTS was observed for the lower heat input, for the UTS a strict correlation with the heat flow cannot be determined. This is mainly due to two factors. First, the presence of hot cracks on the outer surface of wires for which the combination of heat input and low extrusion rate resulted in an excess of heat. Hot cracks do not affect the HV measured "inside" the cross-section, while they have detrimental effects on the tensile properties of the wires. This is the case, as an example, of the wire produced with R = 500 rpm and F = 15 kN, as shown in Fig. 8b, for which the most severe conditions were observed due to the combination of high tool rotation and low force resulting in low extrusion rate.

Also, even for hot cracking-free wires, the outer surface can be considered a "weaker" area for all wires and rods produced by FSE [27, 32]. However, due to the small diameter of the wire here considered, this aspect could not be highlighted by the HV measurements. Finally, it is observed that a nearly monotonic trend of HV with the heat flows implies that, for the input process parameters considered in this study, no detrimental effect of excessive grain growth occurs.

Figure 9 shows the etched cross-section of all the considered case studies.

For all the wires produced with force equal to 15 kN, the cross-section was not perfectly round, and inconsistent geometry was found along the wire axis, consistently with the results obtained from the tensile tests and the observations made. As it will be better highlighted with the numerical results, this depends on two different factors: the insufficient bonding conditions reached due to low tool rotation, for case study 1, and the hot cracking, as discussed for case study 3.
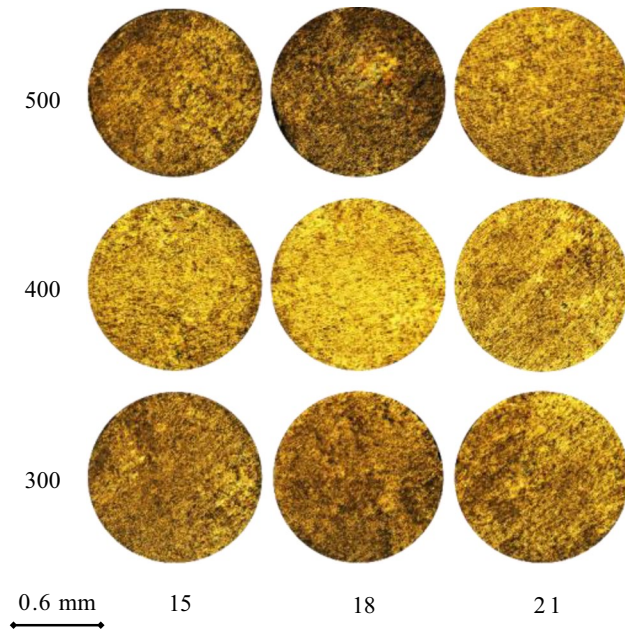
Fig. 9 Etched cross-section of the considered case studies

Fig. 10 Minimum bending radius reached for case studies 2 and 5

3.3 Process Parameters Effect on Material Flow

Figures 11, 12, and 13 show the calculated distribution of temperature, strain, and strain rate, respectively, in a cross-section. Case studies 1, 5, and 9, corresponding to the highest, intermediate, and lowest heat flow, respectively, are presented.

It is noted that the higher heat flow results, as expected, in higher temperatures. Besides, both the increased tool velocity and the enhanced softening of the material, caused by the high temperature, determine higher values of strain and strain rate. Although a detailed study of the occurring bonding condition through the Piwnik and Plata criterion was not carried out in this study, it can be stated that these three conditions favor the solid bonding between the chips. On the contrary, for case study 1, i.e., the one obtained with tool rotation equal to 300 rpm and tool force equal to 15 kN, the maximum temperature hardly reaches 300 °C in the extruded wire, making it almost impossible for sound bonding to occur. Additionally, for case studies 5 and 9, the larger area interested by high deformation before the extrusion channel, suggests that solid bonding occurs before the onset of the actual extrusion process. The same does not apply to case study 1, for which sufficient strain is generated only when the material is in the extrusion channel, leaving less

Finally, bending tests have been carried out. The obtained results are summarized in Table 4.

It is seen that when the extrusion force is equal to 18 kN and 21 kN the minimum bending radius can be obtained, regardless of the tool rotation. On the contrary, when the extrusion force is equal to 15 kN, the wire ductility is significantly reduced: as case study 1 is considered, the poor bonding between the chips resulted in fracture with the largest radius; although the ductility increases with increasing tool rotation, the severe hot cracking previously shown limits also the ductility of case study 3, which fails when bent with a radius equal to 10 mm. Figure 10 shows the bending radius reached for case studies 2 and 5. As the former is considered, a smaller radius resulted in the fracture of the wire.
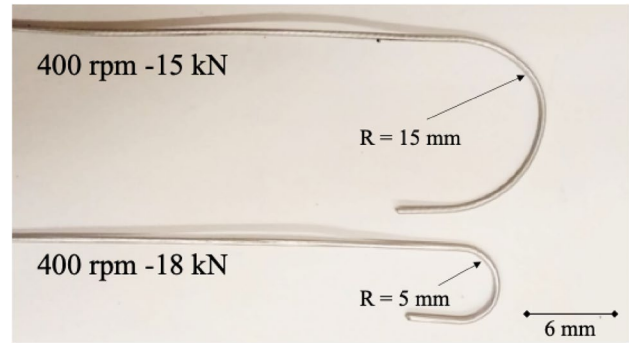
Table 4 Bending test results for the considered case studies

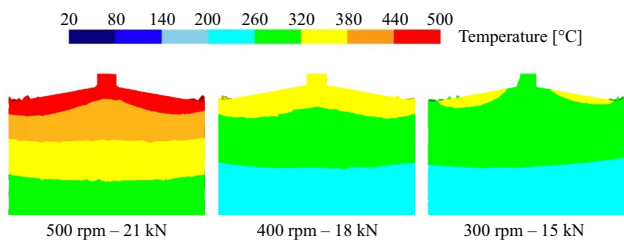| (kN)	(rpm)	Total radius (mm)				
		15	12.5	10	7.5	5
15	300	✗	–	–	–	–
	400	✓	✗	–	–	–
	500	✓	✓	✗	–	–
18	300	✓	✓	✓	✓	✓
	400	✓	✓	✓	✓	✓
	500	✓	✓	✓	✓	✓
21	300	✓	✓	✓	✓	✓
	400	✓	✓	✓	✓	✓
	500	✓	✓	✓	✓	✓

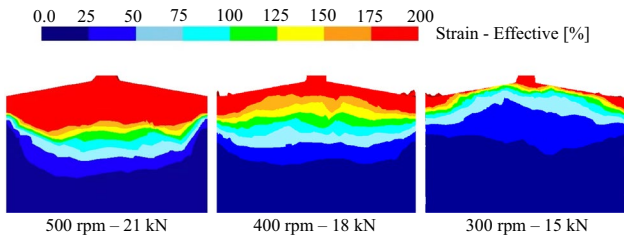**Fig. 11** Temperature distribution in a cross-section for case studies 9, 5, and 1

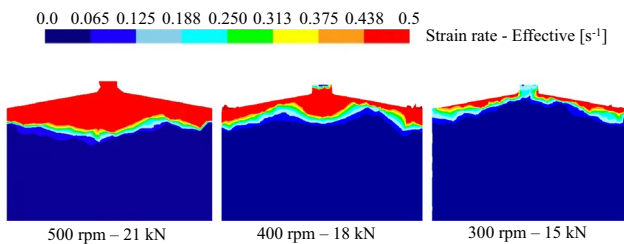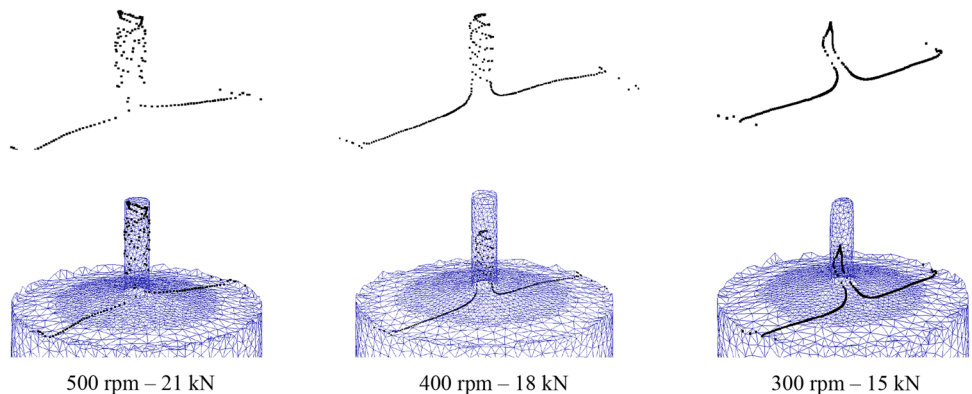**Fig. 12** Effective strain distribution in a cross-section for case studies 9, 5, and 1

Fig. 13 Effective strain rate distribution in a cross-section for case studies 9, 5, and 1

Fig. 14 Material flow for case studies 9, 5, and 1

the material for sound solid bonding [36]. Finally, the material flow is presented for the above-considered case studies. In particular, the position of a set of points of the workpiece initially laying on a diameter in the extrusion chamber was tracked during the process (Fig. 14). It should be noted that while large deformation occurs and adaptive remeshing is triggered during the simulation, the "point tracking" option of the utilized commercial software was used to study the movement of a single particle of material, which, in this way, is not linked to a mesh element. This allows to better analyze the material flow reaching results close to the ones obtainable with a more appropriate smooth particle hydrodynamics simulation [37], keeping at the same time the advantages of a lagrangian approach.

The results highlight how the typical helicoidal flow of FSE is not obtained when tool rotation and tool force are too low. In these conditions, insufficient material mixing results in the poor bonding and the poor mechanical properties previously observed. For the other two case studies, for which UTS larger than the one of the parent materials in the O state and good bending properties were obtained, proper helical movement of material is calculated. It is noted that the pitch of the helix is smaller for case study 5, characterized by higher tool rotation with respect to case study 1. This is because of the opposite effects of tool rotation and tool force. In fact, increasing tool rotation results in lower helix pitch, while increasing force results in increased extrusion rate and, hence, increased pitch. Based on the results obtained, it can be stated that, for the considered process parameters, the effect of tool rotation prevails over the one of force.

3.4 Influence of Process Parameters on Energy Demands

time for the solid bonding to occur. It is worth noticing that, according to the Piwnik and Plata criterion, proper conditions of temperature, pressure, and time must be reached in

In this section the electrical energy demand of the Friction Stir Extrusion process for producing thin wires out

of chips is analyzed. The power-time data were collected by connecting a three-phases electrical networks analyzer to the input electrical connection of the ESAB machine. The power was measured for the entire production cycle, specifically the production of 1000 mm long wire was considered as functional unit. After collecting the power trends, the energy consumption was calculated from the power-time graph by direct numerical integration method. In Fig. 15 the analyzed power trend for the 500 rpm–21 kN process parameters configuration is reported with all the different production modes highlighted. The compaction phase concerns the application of 3 compaction cycles with a vertical load equal to 5 kN. In the transition phase the tool rotation was activated, and the vertical load was gradually increased from 5 kN to the desired load (15, 18, 21 kN). The transition phase is needed as, due to machine limitation, it was not possible to instantly increase the load from 5 kN compaction force to the desired vertical load, hence it must be gradually increased. In Fig. 15 the punch displacement trend is also reported, and it is possible to notice the sudden displacement increase during the transition step due to the increase in chips density caused by both the rotational speed activation as well as by the incremental increasing of the vertical load.
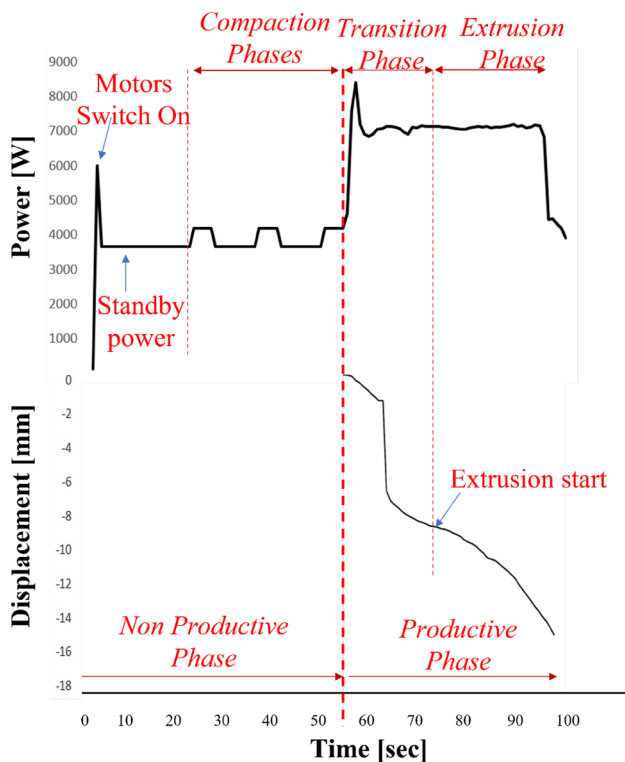

Fig. 15 Power and punch displacement trends (case studies 9)

To calculate this process's energy effectiveness the Specific Energy Consumption (SEC) must be calculated. The SEC (MJ/kg) is a well-recognized indicator [38] for characterizing the energy demand of a manufacturing process and can be used to assess the effectiveness of various process parameters configuration and even different processes one another. In the FSE case, the SEC means the unit energy for producing 1 kg of wire out of aluminum alloys chips.

For the SEC calculation, only the productive phase was considered. In fact, the non-productive phases should be included only when robust industrial practices are considered and clear allocation procedure on the functional unit can be identified. Since our tests were developed in lab environment, and in a discrete production scenario (1000 mm long wires), the selection of the productive phase appears a fair choice. In Table 4 the average power level during the extrusion phase, the SEC and the extrusion rate for 4 different process parameters configurations are reported. The selection reported in Table 5 was driven by the will of analyzing the process parameters configuration characterized by the best mechanical performance as well as by the purpose to observe the impact of the process parameters on the SEC itself. Looking at the results reported in Table 5 it is possible to see that with increasing the vertical load and the rotational speed the SEC decreases. Actually, the efficiency of the processes is governed by the extrusion rate: the higher the extrusion rate, the better the SEC values are. This frequently occurs in manufacturing operations because the shorter processing times effectively outweigh the higher power demands brought on by heavier loads.

Some of the authors of the present paper have already characterized the efficiency of FSE process as used for producing rod (8 mm diameter aluminum alloys wires) [22]. The here identified 102 MJ/kg SEC value for ID9 still provides substantial energy saving with respect the conventional route quantified in that research. More specifically, the saving might be even larger as further wire drawing steps (after hot extrusion in the re-melting rote) might be needed for obtaining the thin wire here considered.

Table 5 Power, extrusion rate (E) and SEC for different process parameters configuration

Case study ID	F (kN)	R (rpm)	Power (W)	E (mm/s)	SEC (MJ/kg)
ID5	18	400	6780.8	15.7	141.2
ID8	21	400	7114.5	20.8	113.8
ID6	18	500	6931.8	16.2	140.3
ID9	21	500	7300.1	24.1	102

4 Conclusions

In the paper, the results of an experimental and numerical study on FSE of thin wires out of AA6082 aluminum alloy machining chips are presented. The study was aimed at the process design to produce wires as filler material in welding and welding-based additive manufacturing processes. For this reason, both standard mechanical tests. i.e., tensile test and HV measurements, and specific tests, i.e., bending tests simulating the wrapping around reels, were carried out. The key findings that may be made from the results are as follows:

- The use of a conical shoulder surface results in higher temperature and strain in the workpiece, which are beneficial for proper solid bonding to occur.
- As the range of process parameters used in this study is regarded, increasing hardness was found with increasing heat flow, which, in turn, increases with tool force and tool rotation.
- HV values between the ones of the parent material in the T4 state and the one in the T6 state are found, suggesting that the process conditions determine a heat treatment in the material with natural aging like the T4 temper.
- UTS values are lower or equal to the one of the parent materials in the T4 state. These values cannot be overcome because of either the hot cracking defects observed or, for defect-free wires, to the "weaker" outer layer which could not be measured in the produced wires due to the small diameter.
- Excellent bending properties are obtained when proper process parameters are selected, which makes the process feasible to produce filler wires wrapped in reels.
- The numerical model results allowed us to explain the mechanical properties obtained with varying input process parameters by showing how temperature, strain, strain rate and material flow improve with increasing tool force and tool rotation.
- The specific energy consumption decreases with increasing tool rotation and tool force. Considering the most efficient process conditions, significant savings can be obtained with respect to conventional production routes.

The good mechanical and microstructural properties observed in the obtained thin wires unlock the potential of FSE to be used also as Symbiotic link enabler. Virtuous output/input links can be activated between chips recycler and wire based Additive Manufacturing/fusion welding companies. In conclusion, along with the energy saving for the aluminum secondary production, further reductions can be obtained by brand new Industrial Symbiosis link activation.

Future works include the extension of the process parameters ranges and the concurrent analysis of the actual bonding conditions through the Piwnik and Plata criterion as well as a detailed microstructural analysis highlighting recrystallization and grain growth phenomena. Further development will concern a full Life Cycle Assessment implementation, including industrial practices, to identify the correct process steps for turning chips into these wires in different production routes (conventional and Solid State based).

References

1. Li, H., Wu, Y., Cao, H., Lu, F., & Li, C. (2022). Energy dissipation characteristics modelling for hot extrusion forming of aluminum-alloy components. *International Journal of Precision Engineering and Manufacturing Green Technology, 9*(6), 1439–1461. https://doi.org/10.1007/S40684-021-00410-Y

2. Sanyé-Mengual, E., Secchi, M., Corrado, S., Beylot, A., & Sala, S. (2019). Assessing the decoupling of economic growth from environmental impacts in the European Union: A consumption-based approach. *Journal of Cleaner Production, 236*, 117535. https://doi.org/10.1016/J.JCLEPRO.2019.07.010

3. Hennicke, P., Khosla, A., Dewan, C., Nagrath, K., Niazi, Z., O'brien, M., & Wilts, H. (2014). Decoupling economic growth from resource consumption a transformation strategy with manifold sociooeconomic benefits for India and Germany. Retrieved from www.schumacher-visuell.de

4. Ingarao, G. (2017). Manufacturing strategies for efficiency in energy and resources use: The role of metal shaping processes. *Journal of Cleaner Production, 142*, 2872–2886. https://doi.org/10.1016/J.JCLEPRO.2016.10.182

5. Xiong, W., Huang, H., Li, L., Gan, L., Zhu, L., & Liu, Z. (2022). Energy consumption evaluation in stamping workshops via a discrete event simulation-based approach. *International Journal of Precision Engineering and Manufacturing Green Technology, 9*(6), 1543–1562. https://doi.org/10.1007/S40684-021-00411-X

6. Otani, L. B., Matsuo, M. M., Freitas, B. J. M., Zepon, G., Kiminami, C. S., Botta, W. J., & Bolfarini, C. (2019). Tailoring the microstructure of recycled 319 aluminum alloy aiming at high

ductility. *Journal of Materials Research and Technology-JMR&T, 8*(4), 3539. https://doi.org/10.1016/J.JMRT.2019.06.030

7. Lee, C. M., Choi, Y. H., Ha, J. H., & Woo, W. S. (2017). Eco-friendly technology for recycling of cutting fluids and metal chips: A review. *International Journal of Precision Engineering and Manufacturing Green Technology, 4*(4), 457–468. https://doi.org/10.1007/S40684-017-0051-9

8. Bevilacqua, M., Ciarapica, F. E., Forcellese, A., & Simoncini, M. (2020). Comparison among the environmental impact of solid state and fusion welding processes in joining an aluminium alloy. *Proceedings of the Institution of Mechanical Engineers, Part B: Journal of Engineering Manufacture, 234*(1–2), 140–156. https://doi.org/10.1177/0954405419845572/FORMAT/EPUB

9. Tekkaya, A. E., Schikorra, M., Becker, D., Biermann, D., Hammer, N., & Pantke, K. (2009). Hot profile extrusion of AA-6060 aluminum chips. *Journal of Materials Processing Tech., 7*(209), 3343–3350. https://doi.org/10.1016/J.JMATPROTEC.2008.07.047

10. Haase, M., Ben Khalifa, N., Tekkaya, A. E., & Misiolek, W. Z. (2012). Improving mechanical properties of chip-based aluminum extrudates by integrated extrusion and equal channel angular pressing (iECAP). *Materials Science and Engineering: A, 539*, 194–204. https://doi.org/10.1016/J.MSEA.2012.01.081

11. Paraskevas, D., Vanmeensel, K., Vleugels, J., Dewulf, W., Deng, Y., & Duflou, J. R. (2014). Spark plasma sintering as a solid-state recycling technique: The case of aluminum alloy scrap consolidation. *Materials, 7*(8), 5664. https://doi.org/10.3390/MA7085664

12. Schulze, A., Hering, O., & Tekkaya, A. E. (2022). Production and subsequent forming of chip-based aluminium sheets without remelting. *International Journal of Precision Engineering and Manufacturing Green Technology, 9*(4), 1035–1048. https://doi.org/10.1007/S40684-021-00395-8

13. Cooper, D. R., Song, J., & Gerard, R. (2018). Metal recovery during melting of extruded machining chips. *Journal of Cleaner Production, 200*, 282–292. https://doi.org/10.1016/J.JCLEPRO.2018.07.246

14. Koch, A., Bonhage, M., Teschke, M., Luecker, L., Behrens, B. A., & Walther, F. (2020). Electrical resistance-based fatigue assessment and capability prediction of extrudates from recycled field-assisted sintered EN AW-6082 aluminium chips. *Materials Characterization*. https://doi.org/10.1016/J.MATCHAR.2020.110644

15. Duflou, J. R., Tekkaya, A. E., Haase, M., Welo, T., Vanmeensel, K., Kellens, K., & Paraskevas, D. (2015). Environmental assessment of solid state recycling routes for aluminium alloys: Can solid state processes significantly reduce the environmental impact of aluminium recycling? *CIRP Annals, 64*(1), 37–40. https://doi.org/10.1016/J.CIRP.2015.04.051

16. Rathinasuriyan, C., Pavithra, E., Sankar, R., & Kumar, V. S. S. (2021). Current status and development of submerged friction stir welding: A review. *International Journal of Precision Engineering and Manufacturing Green Technology, 8*(2), 687–701. https://doi.org/10.1007/S40684-020-00187-6

17. Tang, W., & Reynolds, A. P. (2010). Production of wire via friction extrusion of aluminum alloy machining chips. *Journal of Materials Processing Technology, 210*(15), 2231–2237. https://doi.org/10.1016/J.JMATPROTEC.2010.08.010

18. Behnagh, R. A., Mahdavinejad, R., Yavari, A., Abdollahi, M., & Narvan, M. (2014). Production of wire from AA7277 aluminum chips via friction-stir extrusion (FSE). *Metallurgical and Materials Transactions B, 45*(4), 1484–1489. https://doi.org/10.1007/S11663-014-0067-2

19. Tahmasbi, K., & Mahmoodi, M. (2018). Evaluation of microstructure and mechanical properties of aluminum AA7022 produced by friction stir extrusion. *Journal of Manufacturing Processes, 32*, 151–159. https://doi.org/10.1016/J.JMAPRO.2018.02.008

20. Li, X., Reza-E-Rabby, M., Guzman, A., Grant, G., Mathaudhu, S., Hinton, M., & Reynolds, A. (2022). Strain and strain rate in friction extrusion. *Journal of Materials Research and Technology, 20*, 882–893. https://doi.org/10.1016/J.JMRT.2022.07.116

21. Kalsar, R., Ma, X., Darsell, J., Zhang, D., Kappagantula, K., Herling, D. R., & Joshi, V. V. (2022). Microstructure evolution, enhanced aging kinetics, and mechanical properties of AA7075 alloy after friction extrusion. *Materials Science and Engineering: A, 833*, 142575. https://doi.org/10.1016/J.MSEA.2021.142575

22. Baffari, D., Fratini, L., Ingarao, G., Masnata, A., & Reynolds, A. P. (2019). Friction stir extrusion to recycle aluminum alloys scraps: Energy efficiency characterization. *Journal of Manufacturing Processes*, *43*, 63–69. Retrieved from https://pure.unipa.it/en/publications/friction-stir-extrusion-to-recycle-aluminum-alloys-scraps-energy

23. Zhang, H., Zhao, X., Deng, X., Sutton, M. A., Reynolds, A. P., McNeill, S. R., & Ke, X. (2014). Investigation of material flow during friction extrusion process. *International Journal of Mechanical Sciences, 85*, 130–141. https://doi.org/10.1016/J.IJMECSCI.2014.05.011

24. Zhang, H., Li, X., Tang, W., Deng, X., Reynolds, A. P., & Sutton, M. A. (2015). Heat transfer modeling of the friction extrusion process. *Journal of Materials Processing Technology, 221*, 21–30. https://doi.org/10.1016/J.JMATPROTEC.2015.01.032

25. Zhang, H., Li, X., Deng, X., Reynolds, A. P., & Sutton, M. A. (2018). Numerical simulation of friction extrusion process. *Journal of Materials Processing Technology, 253*, 17–26. https://doi.org/10.1016/J.JMATPROTEC.2017.10.053

26. Li, L., Gupta, V., Li, X., Reynolds, A. P., Grant, G., & Soulami, A. (2022). Meshfree simulation and experimental validation of extreme thermomechanical conditions in friction stir extrusion. *Computational Particle Mechanics, 9*(4), 789–809. https://doi.org/10.1007/S40571-021-00445-7/FIGURES/20

27. Baffari, D., Buffa, G., Campanella, D., Fratini, L., & Reynolds, A. P. (2017). Process mechanics in friction stir extrusion of magnesium alloys chips through experiments and numerical simulation. *Journal of Manufacturing Processes, 29*, 41–49. https://doi.org/10.1016/J.JMAPRO.2017.07.010

28. Abdi Behnagh, R., Samanta, A., Agha Mohammad Pour, M., Esmailzadeh, P., & Ding, H. (2019). Predicting microstructure evolution for friction stir extrusion using a cellular automaton method. *Modelling and Simulation in Materials Science and Engineering, 27*(3), 035006. https://doi.org/10.1088/1361-651X/AB044B

29. Liu, G., Bangs, C. E., Müller, D. B., Liu, G., Bangs, C. E., & Müller, D. B. (2013). Stock dynamics and emission pathways of the global aluminium cycle. *NatCC, 3*(4), 338–342. https://doi.org/10.1038/NCLIMATE1698

30. Han, S. W., Yoo, H., Shin, S., Kim, H., Lee, G., Jeon, J., & Cho, J. (2023). Parameter optimization of WAAM with pulsed GMAW for manufacturing propeller-shaped blade. *International Journal of Precision Engineering and Manufacturing*. https://doi.org/10.1007/S12541-023-00797-5

31. Baffari, D., Reynolds, A. P., Li, X., & Fratini, L. (2017). Influence of processing parameters and initial temper on friction stir extrusion of 2050 aluminum alloy. *Journal of Manufacturing Processes, 28*, 319–325. https://doi.org/10.1016/J.JMAPRO.2017.06.013

32. Baffari, D., Buffa, G., & Fratini, L. (2017). A numerical model for Wire integrity prediction in friction stir extrusion of magnesium alloys. *Journal of Materials Processing Technology, 247*, 1–10. https://doi.org/10.1016/J.JMATPROTEC.2017.04.007

33. Buffa, G., Hua, J., Shivpuri, R., & Fratini, L. (2006). Design of the friction stir welding tool using the continuum based FEM model. *Materials Science and Engineering: A, 419*(1–2), 381–388. https://doi.org/10.1016/J.MSEA.2005.09.041

34. Buffa, G., Fratini, L., Impero, F., Masnata, A., Scherillo, F., & Squillace, A. (2020). Surface and mechanical characterization of stationary shoulder friction stir welded lap joints: Experimental and numerical approach. *International Journal of Material Forming, 13*(5), 725–736. https://doi.org/10.1007/S12289-020-01574-9

35. Song, M., & Kovacevic, R. (2003). Thermal modeling of friction stir welding in a moving coordinate system and its validation. *International Journal of Machine Tools & Manufacture, 43*, 605–615. https://doi.org/10.1016/S0890-6955(03)00022-1

36. Plata, M., & Piwnik, J. (2000). Theoretical and experimental analysis of seam weld formation in hot extrusion of aluminum alloys. *Proceedings of International Aluminum Extrusion Technology Seminar*. Retrieved March 15, 2023

37. Tartakovsky, A., Grant, G., Sun, X., & Khaleel, M. (2006). Modeling of friction stir welding (FSW) process with smooth particle hydrodynamics (SPH). *SAE Technical Papers*. https://doi.org/10.4271/2006-01-1394

38. Wippermann, A., Gutowski, T. G., Denkena, B., Dittrich, M. A., & Wessarges, Y. (2020). Electrical energy and material efficiency analysis of machining, additive and hybrid manufacturing. *Journal of Cleaner Production, 251*, 119731. https://doi.org/10.1016/J.JCLEPRO.2019.119731

Davide Campanella received his Ph.D. in Production Engineering from the University of Palermo in 2014. Currently, he is an Assistant professor (RTD-B) of Manufacturing at the University of Palermo. He has collaborated with various research groups in the sector belonging to both Italian and foreign universities. He is a co-author of more than 57 papers, published in peer-reviewed international journals and conference proceedings, book chapters, and a patent. His Research Focus on Methods, solutions, and numerical models for the solid-state joining process and the forming of metallic materials.

Muhammad Adnan is a PhD student in "Mechanical, Manufacturing, Management and Aerospace Innovation" at the University of Palermo. He received his Master degree in Mechanical Engineering from Dalian University of Technology (DUT) China in 2021 and Bachelor Degree from University of Engineering and Technology (UET) Lahore Pakistan in 2018. His Research Focus on Methods, solutions, and numerical models for the solid-state Recycling Process (FSE) and solid-state joining process (FSW).

Gianluca Buffa received his Ph.D. in Industrial and Production Engineering from the University of Palermo in 2007. Currently he is full professor of Manufacturing at University of Palermo. He is coauthor of more than 150 papers, published in peer reviewed international journals and conference proceedings, book chapters and a patent. Dr. Buffa has been awarded with the ESAFORM Scientific prize in 2013. In 2009 he has been awarded as "Best young researcher" at the 9th A.I.Te.M. (Italian Manufacturing Association) Conference. In 2005 dr. Buffa has been awarded at the NAMRC conference for his presentation.

Umberto La Commare Born in Palermo on March 31st, 1956, Prof. Umberto La Commare graduated in Mechanical Engineering in 1980. From 1987 to 1990 he was full professor of Manufacturing at the University of Napoli, since 1990 he is full professor of Manufacturing at the University of Palermo holding now the courses of Operation Management and Management of Technological Innovation. The scientific activity has been mainly focused on mechanical production systems and processes environment. He has been in charge of the technology transfer through spin off of the University of Palermo.

Giuseppe Ingarao received a M.Sc. degree in Management Engineering and a Ph.D. in Industrial Engineering and Management from University of Palermo. He is currently Associate Professor of Manufacturing in the Department of Engineering of University of Palermo. His research focuses on sustainable manufacturing. Specifically, he deals with the design of energy- and resource-efficient metal shaping processes (additive, subtractive and mass conserving), methods and techniques for Life Cycle Assessment of metal components, and innovative metal recycling processes.

Livan Fratini Born in Palermo on October 9th, 1970, Prof. Livan Fratini graduated with honours in Mechanical Engineering in 1993 and took his PhD in Production Engineering in 1997. Currently he is professor to the Chair of Manufacturing at the University of Palermo. He was awarded a young researcher travel award by the Japan Society for Technology of Plasticity (2000) and the F.W. Taylor Medal by the CIRP (2007). Prof. Fratini has been involved in several research projects on metal forming topics. Prof. L. Fratini is coauthor of about 260 papers on international scientific journals.